Cooperative Dispatch of Distributed Energy Storage in Distribution Network With PV Generation Systems

Xiangjun Li, *Senior Member, IEEE*, Lijun Wang, Ning Yan, and Rui Ma

***Abstract*—Battery energy storage system (BESS) plays an important role in solving problems in which the intermittency has to be considered while operating distribution network (DN) penetrated with renewable energy. Aiming at this problem, this paper proposes a global centralized dispatch model that applies BESS technology to DN with renewable energy source (RES). The method proposed in this paper aims to minimize the power purchase cost considering network active loss cost as well as voltage deviation penalty cost. Later, second-order cone programming (SOCP) method as well as big M method are applied to make the problem tractable. Last, the method illustrated in this paper is applied and validated on a modified IEEE 33-bus benchmark system to verify the effectiveness of the proposed scheduling model.**

***Index Terms*—Energy storage, distributed photovoltaic power generation, peak shaving, voltage regulation, economic effect.**

I. Introduction

AROUND the world, renewable energy penetration rate is increasing rapidly, especially, in the case of China. By the end of 2020, China's installed renewable energy capacity has reached 934 000 MW, an increase of 17.5% year-on-year. However, the uncertainty of renewable energy output has brought certain challenges to the operating of DN [1]. BESS, as a flexible resource, plays an important role in operating system highly penetrated with intermittent renewable energy [2], [3]. With the increase of the installed capacity of BESS, it is very necessary to come up with a global centralized operation method of DN that can utilize the flexibility of BESS [4], [5].

At present, there have been many researches on DN scheduling considering ESS [6]–[8]. However, in some research, the ESS scheduling goal of renewable energy side is single, which makes it difficult to reflect the cooperative scheduling effect of BESS and other units in DN. Some researches do not consider network loss, and there is a common problem, that is, network loss cost and voltage deviation cost are not considered simultaneously in the objective function. With the gradual improvement of power auxiliary service market, BESS will also play an important role in power quality management [9], [10], which has a lot of value to explore.

In this paper, a global centralized dispatch model is proposed for DN penetrated with RES and BESS. Under the premise of considering network loss, the proposed model seeks to jointly minimize electricity purchasing cost, active line loss, as well as voltage deviation. Later, to ensure the tractability of the proposed model, second-order cone relaxation technique and big M method are being applied and later the model is being solved by Cplex solver. Last, the result is being evaluated from three major perspectives, peak shaving, voltage regulation, as well as economic effect.

II. Global Centralized Dispatch Model

A. Objective Function

The objective of the DN economic dispatch model with distributed ESS and photovoltaic(PV) power stations is to minimize the sum of the main network purchase cost, the network active loss cost, and the voltage deviation penalty cost, as shown in (1).

$$C_{\min} = \min \left(\sum_t C_{gt} P_{gt} + C_e \sum_{i=1}^{N_{\text{bus}}} \sum_{j\in c(i)} r_{ij} (I_{ij})^2 + C_a \sum_{i,t} |V_{it} - 1| \right) \tag{1}$$

where $C_{\min}$ is the minimum value of t objective function; C_{gt} is the real-time electricity price for main power grid; P_{gt} is the active power provided by the main network to the DN; C_e is the compensation coefficient of network active loss; N_{bus} is the number of network buses; i, j are network buses numbers; $c(i)$ is a set of buses connected with i as a starting point; r_{ij} is branch resistance; I_{ij} is branch current; C_a is the voltage deviation penalty coefficient; V_{it} is voltage magnitude of bus i.

B. Constraint Condition

1) Power balance constraint

Fig. 1 shows part of a DN topology; the power injected or absorbed at each bus and power flow at each branch should

Manuscript received March 13, 2021; revised June 3, 2021 and June 29, 2021; accepted July 13, 2021. Date of publication October 6, 2021; date of current version October 22, 2021. This work was supported in part by the Open Fund of State Key Laboratory of Operation and Control of Renewable Energy & Storage Systems (China Electric Power Research Institute) (No.DGB51202001510).
(Corresponding author: Xiangjun Li.)

Xiangjun Li and Rui Ma are with the State Key Laboratory of Operation and Control of Renewable Energy & Storage Systems, China Electric Power Research Institute, Beijing 100192, China (e-mail: li_xiangjun@126.com; merry0111@163.com).

Lijun Wang and Ning Yan are with the School of Electrical Engineering, Shenyang University of Technology, Shenyang 110870, China (e-mail: 872357172@qq.com; sutxny_yn@126.com).

Color versions of one or more figures in this article are available at https://doi.org/10.1109/TASC.2021.3117750.

Digital Object Identifier 10.1109/TASC.2021.3117750

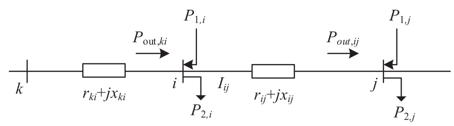

Fig. 1. Diagram for power flow direction of nodes and branches.

satisfy the following power balancing constraints:

$$\begin{cases} \sum\limits_{ki \in N_{bus}} P_{kit} - \sum\limits_{ij \in N_{bus}} P_{ijt} - P_{ijt}^{loss} + P_{it}^{bess} + P_{it}^{gf} = P_{it}^{bus} \\ \sum\limits_{ki \in N_{bus}} Q_{kit} - \sum\limits_{ij \in N_{bus}} Q_{ijt} - Q_{ijt}^{loss} + Q_{it}^{bess} + Q_{it}^{gf} = Q_{it}^{bus} \end{cases} \tag{2}$$

where P_{kit}, Q_{kit} are the active and reactive power flowing into bus i on branch ki; $P_{ijt,}$ Q_{ijt} are the active and reactive power flowing out from bus i on branch ij; P_{ijt}^{loss}, Q_{ijt}^{loss} are the network branch loss for active and reactive power; P_{it}^{bess}, Q_{it}^{bess} are active and reactive power by the ESS i; P_{it}^{gf}, Q_{it}^{gf} are active and reactive power by PV power station i; P_{it}^{bus}, Q_{it}^{bus} are the active and reactive load power of bus i.

2) Voltage drop constraint is (3).

$$(V_{jt})^2 = (V_{it})^2 - 2(r_{ij}P_{ijt} + x_{ij}Q_{ijt}) + ({r_{ij}}^2 + {x_{ij}}^2)I_{ijt}^2 \tag{3}$$

where V_{jt} and V_{it} are the voltage magnitude of bus j and i.

3) Transmission limit constraint is (4).

$$\left\| \begin{matrix} P_{ijt} - I_{ijt}^2 r_{ij} \\ Q_{ijt} - I_{ijt}^2 x_{ij} \end{matrix} \right\| \le S_{ij}^{cap} \tag{4}$$

where S_{ij}^{cap} is the branch transmission capacity.

4) Voltage drop constraint is (5).

$$V_{it}^2 \le \frac{P_{ijt}^2 + Q_{ijt}^2}{I_{ijt}^2} \tag{5}$$

5) Load capacity constraint of ESS is (6).

$$\begin{aligned} &\left\| \begin{matrix} P_{it}^{bess} & \\ & Q_{it}^{bess} \end{matrix} \right\| \le C_{i,\max}^{bess} \\ &P_{it}^{bess} = P_{it}^{Des} - P_{it}^{Ces} \\ &0 \le P_{it}^{Des} \le U_{it}^{bess} C_{\max}^{bess} \\ &0 \le P_{it}^{Ces} \le U_{it}^{bess} C_{\max}^{bess} \\ &0 \le E_{it}^{bees} \le C_{i,\max}^{bess} \\ &E_{it}^{bees} = E_{it-1}^{bees} + \eta_c P_{it}^{Ces} - P_{it}^{Des}/\eta_d \\ &E_{iT}^{bees} = E_{i0}^{bess} \end{aligned} \tag{6}$$

where $C_{i,\max}^{bess}$ is the maximum value of i capacity of the ESS; P_{it}^{Des} is active power discharged by BESS i; P_{it}^{Ces} is active power for charging ESS i; U_{it}^{bess} is a binary variable; E_{it}^{bees} is the remaining power quantity of BESS i; $\eta_c$and $\eta_d$are the charging and discharging efficiency for BESS.

6) Charge and discharge power constraints of PV power station are (7).

$$\begin{cases} 0 \le P_{it}^{gf} \le P_{pvs} \\ 0 \le Q_{it}^{gf} \le Q_{pvs} \end{cases} \tag{7}$$

where P_{pvs} and Q_{pvs} are the maximum active and reactive power provided by photovoltaic power station i.

7) Power constraints by the main network are (8).

$$\begin{cases} 0 \le P_{gt} \le P_{h,max} \\ 0 \le Q_{gt} \le Q_{h,max} \end{cases} \tag{8}$$

where $P_{h,max}$ and $Q_{h,max}$ are the maximum active and reactive power provided by the main network to the DN.

C. Constraint Condition

Using the second-order cone relaxation technique[2], the square of branch current is defined as $i_{2,ij}$ and the square of node voltage amplitude is defined as $u_{2,ij}$, then the linearized conversion can be found as (9)-(13).

$$\begin{cases} u_{2,i} = V_i^2 \\ i_{2,ij} = I_{ij}^2 = \frac{P_{ij}^2 + Q_{ij}^2}{u_{2,i}} \end{cases} \tag{9}$$

(1) It can be converted to

$$C_{\min} = \min \left(\sum_t C_{gt} P_{gt} + C_e \sum_{i=1}^{N_{\text{bus}}} \sum_{j \in c(i)} r_{ij} i_{2,ij} + C_a \sum_{i,t} |V_{it} - 1| \right) \tag{10}$$

(3) It can be converted to

$$u_{2,jt} = u_{2,it} - ({r_{ij}}^2 + {x_{ij}}^2) i_{2,ijt} \tag{11}$$

(4) It can be converted to

$$\left\| \begin{matrix} P_{ijt} - i_{2,ijt} r_{ij} \\ Q_{ijt} - i_{2,ijt} x_{ij} \end{matrix} \right\| \le S_{ij}^{cap} \tag{12}$$

(5) It can be converted to

$$\left\| [2P_{ijt} 2Q_{ijt} \mathrm{i}_{2,ijt} - u_{2,ijt}]^{\mathrm{T}} \right\|_2 \le \mathrm{i}_{2,ijt} + u_{2,ijt} \tag{13}$$

The absolute value sign in (1) can be removed by introducing binary variables, and when $(V_{it} - 1)$ is non-negative, it is 1; When $(V_{it} - 1)$ is negative, it is 0. (14) can be expressed linearly by the big M method as follows:

$$\begin{aligned} &(2\alpha_{it} - 1)(V_{it} - 1) = 2v_{it}^p - (V_{it} - 1) \\ &0 \le v_{it}^p - (V_{it} - 1) \le M(1 - \alpha_{it}) \\ &0 \le v_{it}^p \le M\alpha_{it} \end{aligned} \tag{14}$$

Continuous variables $\alpha_{it}(V_{it} - 1)$ were used v_{it}^p instead. When α_{it} is 0, v_{it}^p is 0, and $(V_{it} - 1)$ is negative; When α_{it} is 1, $v_{it}^p = (V_{it} - 1)$, and $(V_{it} - 1)$ is not negative.

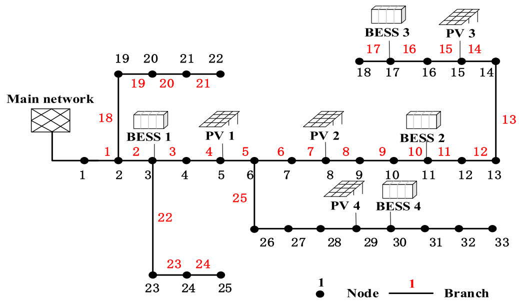

Fig. 2. The topology of the modified IEEE 33-node system.

TABLE I
THE PARAMETERS OF BESSs AND PV STATIONS

Station	Installed node	Installed capacity (MW)
BESS 1	3	2
BESS 2	11	1
BESS 3	17	1
BESS 4	30	2
PV 1	5	2
PV 2	8	1
PV 3	15	1
PV 4	29	2

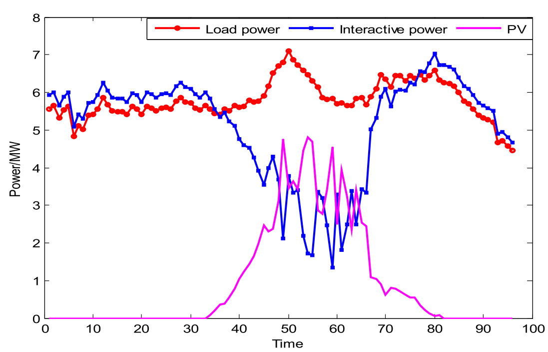

Fig. 3. Output of units without BESSs.

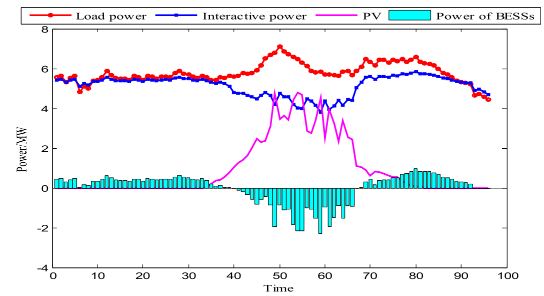

Fig. 4. Output of units with BESSs.

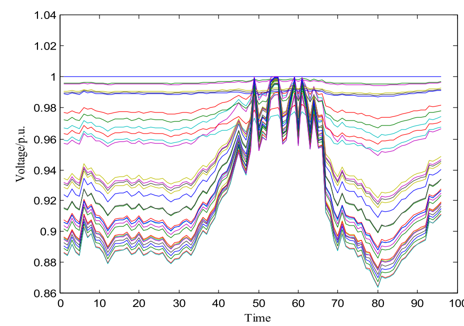

Fig. 5. Voltage profiles of nodes without BESSs.

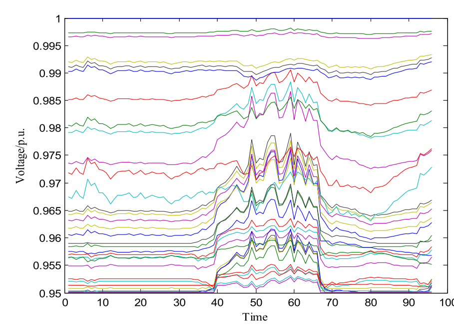

Fig. 6. Voltage profiles of nodes with BESSs.

III. CASE STUDY

A modified IEEE 33-node system has been used to simulate and verify the proposed model. The topology of the modified IEEE 33-node system is shown in Fig. 2.

As can be seen from Fig. 2, IEEE 33-node test system consists of 33 buses and 32 branches. Four BESSs and four PV stations are connected to the DN. In order to follow the principle of power generation and use nearby, BESSs and PV stations are distributed, the parameters of DN are shown in Table I. The time interval is set to 15 min and a day is divided into 96 time periods.

A. Analysis of Peak Shaving Effect of BESS

BESS can mitigate PV intermittency through energy throughput and auxiliary power peak shaving. In this paper, the PV rejection rate of BESS before and after participating in dispatching is compared, and the effectiveness of ESS technology to improve the system's ability to accept PV and participate in power peak shaving is analyzed. Output of units without BESSs is shown in Fig. 3. Output of units with BESSs is shown in Fig. 4.

By comparing Fig. 3 and Fig. 4, we can see that in the time periods of 0-39 and 68-92, the interactive power between the system and the transmission network is significantly reduced due to the power released by BESSs. In the time period of 68-92, the energy storage device releases power, which makes the output curve of interactive power more smooth. At the same time, after applying BESSs, the PV rejection rate decreased significantly from 28.7% to 8.4%.

B. Analysis of Voltage Regulation Effect of BESS

Voltage profiles of nodes without BESSs is shown in Fig. 5 and voltage profiles of nodes with BESSs is shown in Fig. 6.

By comparing Fig. 5 and Fig. 6, we can see that under the regulation of the BESSs, the low-voltage problem of the system during the peak period of night load is solved. At the same time, we can see that the node voltage reaches the lowest at 8:00 p.m. in a day, so 8:00 p.m. are selected as typical time when the system has no access to energy storage to investigate the improvement of the system node voltage with and without BESSs. The node voltage distribution diagram at the typical time is shown in Fig. 7.

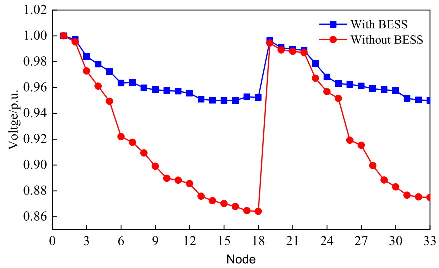

Fig. 7. Node voltage distribution at typical time.

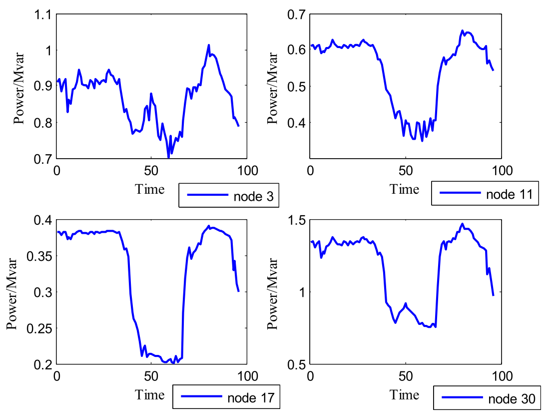

Fig. 8. The reactive power variations of BESSs.

TABLE II
THE COMPARISON OF SYSTEM SCHEDULING COSTS

Cost/Yuan	Without BESSs	With BESSs
Power purchase by main network	132436	129656
Network active loss	2665.8	2374
Voltage deviation penalty	3286.3	2118.5
Total cost	138388.1	134148.5

As can be seen that after the BESSs are connected, the voltage of each node increases significantly, and the voltage deviation is controlled within the allowable range. The minimum voltage increases from 0.864 to 0.95 p. u. and the voltage qualification rate of the system increases from 33.3% to 100%.

Fig. 8 shows the reactive power variations of each BESS in a day. It can be seen that reactive power absorption occurs more in the morning and evening, less in the afternoon. This indicates that there is a certain redundancy of reactive power near node which BESSs are connected with during daytime, thus the node voltage is high.

C. Analysis of Economic Effect of BESS

Table II shows the comparison of system scheduling costs with or without BESSs, the cost calculation formula is shown in Formula 1.

As we can see, through coordinated dispatching of BESSs, the total cost is reduced from 138388.1 Yuan to 134148.5 Yuan, and the overall economy is improved by 3.1%.

IV. CONCLUSION

An cooperative dispatch method for distributed energy storage in DN with PV power generation systems has been presented in the paper. The second-order cone relaxation technique and the big M method are used to linearize the model. The proposed model and solution technique are validated using the modified IEEE 33-node system. The conclusions are drawn as follows.

The power output characteristics of each time point are obtained by using the solution of Cplex. The solution is simple and fast, and it is suitable for solving multi-objective optimization and control problems. BESS can significantly improve the peak shaving capacity of the system. For the IEEE 33-node system, it can reduce the system's PV abandonment rate from 28.7% to 8.4%.BESS can significantly improve the voltage regulation capacity of the system. The minimum voltage increases from 0.864 to 0.95 p. u. BESS can improve the economics of the system operation. The overall economy is improved by 3.1%.

REFERENCES

[1] V. V. S. N. Murty and A. Kumar, "Multi-objective energy management in microgrids with hybrid energy sources and battery energy storage systems," *Protection Control Modern Power Syst.*, vol. 5, no. 1, pp. 1–20, 2020.

[2] X. Li, L. Wang, N. Yan, and R. Ma, "Economic dispatch of distribution network with distributed energy storage and PV power stations," in *Proc. IEEE Int. Conf. Appl. Supercond. Electromagn. Devices*, Oct. 2020, pp. 1–2.

[3] S. Zhang, J. Wang, and H. Liu, "Prediction of energy photovoltaic power generation based on artificial intelligence algorithm," *Neural Comput. Appl.*, vol. 33, no. 1, pp. 821–835, 2020.

[4] J. Zhang *et al.*, "Analysis of the development of energy storage market and the key development direction in China," *Power Energy*, vol. 41, no. 6, pp. 739–743, 2020.

[5] J. Wang, X. Chen, F. Zhang, F. Chen, and Y. Xin, "Building load forecasting using deep neural network with efficient feature fusion," *J. Modern Power Syst. Clean Energy*, vol. 9, no. 1, pp. 160–169, 2021.

[6] X. Li and S. Wang, "A review on energy management, operation control and application methods for grid battery energy storage systems," *CSEE J. Power Energy Syst.*, vol. 99, pp. 1–15, 2019, doi: 10.17775/CSEE-JPES.2019.00160.

[7] W. Gan, J. Guo, X. Li, and J. Wen, "Distributed energy storage optimization scheduling for multiple application requirements," *Power System Technol.*, vol. 43, no. 5, pp. 1504–1511, 2019.

[8] Z. Wang, H. Lin, and Y. Ma, "A control strategy of modular multilevel converter with integrated battery energy storage system based on battery side capacitor voltage control," *Energies*, vol. 12, no. 11, pp. 2151–2170, 2019.

[9] X. Li *et al.*, "Multi-timescale cooperated optimal dispatch strategy for ultra-large-scale storage system," *Energy Rep.*, vol. 6, pp. 1–8, 2020.

[10] F. Yao, J. Zhao, X. Li, L. Mao, and K. Qu, "RBF neural network based virtual synchronous generator control with improved frequency stability," *IEEE Trans. Ind. Inform.*, vol. 17, no. 6, pp. 4014–4024, Jun. 2021.